Available online at www.sciencedirect.com
ScienceDirect
Journal of Hazardous Materials 152 (2008) 1130–1137
Journal of Hazardous Materials
www.elsevier.com/locate/jhazmat

Bromide ion removal from contaminated water by calcined and uncalcined MgAl-CO_3 layered double hydroxides

Liang Lv [a,*], Yulin Wang [a], Min Wei [b], Jianjun Cheng [a]

[a] West Branch of Zhejiang University of Technology, Zhejiang 324006, China
[b] Key Laboratory of Science and Technology of Controllable Chemical Reactions, Ministry of Education, Beijing University of Chemical Technology, Beijing 100029, China

Received 14 September 2006; received in revised form 26 July 2007; accepted 27 July 2007
Available online 8 August 2007

Abstract

A fundamental investigation on the uptake of bromide ion from contaminated water by calcined and uncalcined MgAl-CO_3 layered double hydroxides (LDHs) were conducted in batch mode. The uptake capacity of calcined LDHs (CLDH) is higher than that of uncalcined LDHs, due to their different mechanisms which are confirmed by powder X-ray diffraction, FT-IR spectroscopy and TG–MS measurements. The former mechanism is based on the reconstruction of CLDH to Br-LDHs, whilst the latter is related to the surface adsorption. It has been found that the LDHs calcined at 500 °C with Mg/Al molar ratio of 4 represents the highest capacity to remove bromide ion from aqueous solution. The equilibrium isotherms of uptake of bromide by CLDH were well fitted by the Langmuir equation, and thermodynamic parameters such as ΔG^0, ΔH^0 and ΔS^0 were calculated from Langmuir constants. The negative value of ΔH^0 confirms the exothermic nature of adsorption. Three kinetics models were used to fit the kinetics experimental data, and it was found that the pseudo-second order kinetics model could be used to describe the uptake process appropriately. The value of E_a was calculated to be 79.9 kJ/mol, which suggests that the process of uptake bromide is controlled by the reaction rate of bromide with the CLDH rather than diffusion.
© 2007 Elsevier B.V. All rights reserved.

Keywords: Layered double hydroxides; Calcined; Bromide; Removal; Equilibrium; Kinetics

1. Introduction

Layered double hydroxides (LDHs) or hydrotalcite-like compounds (HTlc) can be represented by the general formula $[M^{2+}_{1-x}M^{3+}_x(OH)_2]^{x+}(A^{n-})_{x/n}\cdot mH_2O$, where M^{2+} and M^{3+} are di- and trivalent metal cations for example Mg^{2+} and Al^{3+}, that occupy octahedral sites in the hydroxide layers. A^{n-} is an exchangeable anion, and x is the ratio of $M^{3+}/(M^{2+}+M^{3+})$ and the layer charge will depend on the M^{2+}/M^{3+} ratio [1]. Carbonates are the interlayer anions in naturally occurring hydrotalcite. LDHs have large surface area (20–120 m^2/g) and high ion-exchange capacities to adsorb/ion-exchange the variety of anionic pollution. On the other hand, the LDHs decompose at 500–800 °C to a magnesium–aluminium oxide solid solution which rehydrates and reconstructs the original structure from water containing anions [2], and hence could also be a potential adsorbent for anionic solutes. Calcined layered double hydroxide (CLDH) is an especially exciting adsorbent because it has the potential to remove fluoride, chloride, and other anions toxic anions from contaminated water [3–9].

Bromide is a natural, albeit minor, constituent of all waters. Bromide concentrations in water depend primarily on the geochemistry of the materials in which the water has come into contact [10]. High bromide concentration is typical in surface and groundwaters in the coastal areas [11]. Although bromide ion is not harmful to human body, it can be converted to bromate (BrO_3^-) which is suspected carcinogenic potential, in drinking water treatment during oxidation and disinfection with ozone. On the other hand, Grignard regents have been applied extensive in chemical industry, especially in pharmacy. A mass of bromide-containing wastewater was produced after reaction, and ozonation these organic contaminants can produce bromate and other brominated pollutants [12,13]. The US Environmental Protection Agency (EPA) has established a maximum contam-

* Corresponding author at: 78 Jiu Hua Shan Lu, Ke Cheng District, Quzhou City, Zhejiang Province, 324000, China. Tel.: +86 570 8510552; fax: +86 570 8026668.
E-mail address: lianglv_qzxy@126.com (L. Lv).

0304-3894/$ – see front matter © 2007 Elsevier B.V. All rights reserved.
doi:10.1016/j.jhazmat.2007.07.117

inant level of 10 μg/L for bromate in finished water [14,15]. Brominated by-products are suspected to be more harmful to health than their chloride-containing analogues [16]. Therefore, it is necessary and significant to removal the DBPs (disinfection by-products) precursor bromide. Enhanced coagulation, a traditional precursor removal strategy, and anion exchange, a more novel precursor removal strategy, are two areas of active research for controlling DBPs formation, which are generally known as nanofiltration membrane processes and activated carbon adsorption processes [17,18].

In this work, the uptake of bromide by calcined and uncalcined MgAl-CO_3 LDHs has been studied. Their different mechanism is confirmed by X-ray diffraction, FT-IR spectroscopy and TG–MS measurements. The kinetics and equilibrium of CLDH on removal bromide have also been investigated in detail. The equilibrium isotherms were fitted by the Langmuir and Freundlich equations, respectively. Furthermore, three kinetics models were used to fit the experimental data, including first order kinetics model, pseudo-second order kinetics model and intraparticle diffusion model, and it was found that the pseudo-second order kinetics model describes the uptake process the most appropriately.

2. Experimental

2.1. Materials

$Mg(NO_3)_2{\cdot}6H_2O$, $Al(NO_3)_3{\cdot}9H_2O$, NaOH, Na_2CO_3, $NaNO_3$, KNO_3 and KBr were A.R. grade and used as received without purification. All the water used was deionized. The bromide aqueous solution used in this study was a synthetic wastewater. The standard bromide solutions used in the experiments were prepared from anhydrous KBr.

2.2. Preparation of MgAl-CO_3 LDHs and CLDH

LDHs containing carbonate as the interlayer anion was obtained by using a conventional coprecipitation method previously developed by our group [19,20]. $Mg(NO_3)_2{\cdot}6H_2O$ (0.36 mol) and $Al(NO_3)_3{\cdot}9H_2O$ (0.09 mol) were dissolved in deionized water. A second solution containing NaOH (0.72 mol) and Na_2CO_3 (0.36 mol) was prepared. The two solutions were simultaneously added to a colloid mill with rotor speed of 5000 rpm and stirred for 2 min. The resulting slurry was removed from the colloid mill and aged at 100 °C for a specified period. The final precipitate was filtered, washed throughly, and dried at 80 °C for 24 h to obtain MgAl-CO_3 LDHs. CLDH was obtained by calcining LDHs in a muffle furnace at 500 °C for 3 h.

2.3. Characterization

Powder X-ray diffraction pattern of the samples were obtained using a Shimadzu XRD-6000 diffractometer with Cu Kα radiation (40 kV and 30 mA) at a scanning rate of 5°/min. FT-IR spectra in the range 4000–400 cm^{-1} of samples as KBr pellets were recorded with a Bruker Vector 22 spectrometer. TG–MS measurements were carried out on a Pyris Diamond TG/DTA instrument equipped with a mass spectrometer (ThermoStar TM) under N_2 atmosphere. The temperature-programmed rate was 10 °C/min, and the measured range from 30 to 1100 °C. Gaseous emission was analyzed at intervals of 1 s. Elemental analysis was performed by inductively coupled plasma (ICP) emission spectroscopy with a Shimadzu ICPS-7500 ICP instrument using solutions prepared by dissolving the samples in dilute HNO_3.

2.4. Removal of bromide ion

All uptake studies were carried out in a series of 100 mL conical flasks by subjecting a given dose of LDHs or CLDH to a period of shaking together with the bromide wastewater (50 mL) in a thermostatic water shaker.

Batch equilibrium isotherms studies on CLDH were conducted with a range of different concentrations of bromide solutions by contacting a constant mass (0.05 g) of CLDH for a period of 24 h at 30, 40, 50, 60 ± 1 °C, using the maximum shaking rate of 200 rpm. After equilibration, CLDH was filtered from the solution, and the filtrate was analyzed using a selective electrode for bromide ions.

The amount of the bromides loading (mg) per unit mass of CLDH, q_e, was obtained by the following equation

$$q_e = (C_i - C_e)\frac{V}{m} \quad (1)$$

where C_i and C_e are initial and equilibrium concentrations in mg/L, m is the mass of adsorbent in grams, and V is the volume of solution in liters.

Kinetic experiments were carried out by dispersing CLDH samples (2.0 g) in 2000 mL of bromide solutions with a concentration of 100 mg Br^-/L and stirred for 6 h under N_2 atmosphere. 5 mL aliquots were extracted at selected time intervals, separated by filtration, and diluted to 50 mL for the determination of Br^-. The solid remaining at the end of the experiment was characterized by X-ray diffraction, FT-IR and TG–MS. Bromide uptake by the CLDH was calculated by the following equation:

$$q_t = (C_i - C_t)\frac{V}{m} \quad (2)$$

where q_t is the adsorption capacity of CLDH at time t in mg/g, V is the volume of solution in liters, C_i and C_t are initial and at time t concentration of bromide in mg/L, and m is the mass of adsorbent in grams.

3. Theory

3.1. Equilibrium isotherms

For the liquid–solid system, the Langmuir and Freundlich isotherm equations are usually employed. The well-known Langmuir equation, which is obtained by combining the adsorption and desorption rate equations, can be described as following

Eq. (3) when the adsorption process reaches equilibrium.

$$q_e = \frac{K_L q_m C_e}{1 + K_L C_e} \quad (3)$$

where $K_L = k_{ads}/k_d$ is the Langmuir constant related to the loading and energy of adsorption; q_m the maximum loading capacity; q_e the adsorption loading at equilibrium (mg/g), and C_e is the equilibrium concentration of bromide in the solution (mg/L).

The langmuir equation can be rearranged as follows:

$$\frac{C_e}{q_e} = \frac{1}{K_L q_m} + \frac{C_e}{q_m} \quad (4)$$

The values of q_m and K_L can be calculated from the slope and the intercept of the linear plots C_e/q_e versus C_e.

The Freundlich isotherm is purely empirical and commonly presented as Eq. (5):

$$q_e = K_F C_e^n \quad (5)$$

where K_F and n are the Freundlich temperature-dependent constants, and q_e is the adsorption loading at equilibrium (mg/g), respectively.

3.2. Distribution coefficient

The distribution coefficient K_D can be employed to describe the binding ability of adsorbent surface for an element. The K_D values of the adsorption were calculated as Eq. (6):

$$K_D = \frac{C_s}{C_w} \quad (6)$$

where C_s is the concentration of bromide in solid particles (mg/g) and C_w is the concentration of bromide in water (mg/L).

3.3. Kinetic models

To identify the correct mechanism, several models must be checked for suitability and consistency over a broad range of system parameters. The key features of the three different kinetic models used to fit the experimental data can be summarized as follows:

3.3.1. First order kinetics model

The first order kinetics adsorption model was suggested by Lagergren for the sorption of solid/liquid systems [21]. It has been used by many authors [22–24] and can be expressed in integrated form:

$$\ln(q_e - q_t) = \ln(q_e) - k_1 t \quad (7)$$

where k_1 is the rate constant of adsorption (min^{-1}) and q_e and q_t are the adsorption capacity of bromide (mg/g) at equilibrium and at time t (min), respectively. The equilibrium capacity q_e (mg/g), is calculated from the Langmuir adsorption isotherm. By plotting $\ln(q_e - q_t)$ against t, a straight line is obtained and the value of the rate constant k_1 can be calculated.

3.3.2. Pseudo-second order kinetics model

The pseudo-second order kinetics model [25,26] is expressed as

$$\frac{t}{q_t} = \frac{1}{k_2 q_e^2} + \frac{t}{q_e} \quad (8)$$

where k_2 ($g\,mg^{-1}\,min^{-1}$) is the rate constant of pseudo-second order adsorption. Plotting t/q_t against t, a line is obtained and the rate constant k_2 as well as q_e can be calculated.

3.3.3. Intraparticle diffusion model

In a liquid–solid system, the fractional uptake of the solute on a particle, F, varies [27,28] with the function $D_0 t^{0.5}/r^2$. Hence there is a linear relationship between F and $t^{0.5}$ for most of the adsorption process. F can be defined as

$$F = \frac{C_i - C_t}{C_i} \quad (9)$$

The diffusion rate of the bromide in a particle, k_i, can be calculated from the following linear equation [29]:

$$q_t = k_i t^{0.5} \quad (10)$$

where k_i is the intraparticle diffusion rate ($mg\,g^{-1}\,min^{-0.5}$).

4. Results and Discussion

4.1. Effect of varying structure of adsorbents

The uptake of bromide ion by the as-synthesized LDHs and LDHs calcined at various temperatures were tested. The adsorption was carried out by dispersing 0.05 g of CLDH in a constant volume of 50 mL bromide ion aqueous solution, with initial concentration of bromide 100 mg/L at 30 °C. The uptake capacity of bromide ion increases with increasing calcination temperature between 200 and 500 °C, but decreases from 500 to 800 °C, with a maximum (94.0 mg/g) for LDHs calcined at 500 °C. The uptake capacity of bromide ion by uncalcined LDHs (27.5 mg/g) is the lowest of all. This result is consistent with the structure transformation of LDHs upon calcination. When LDHs is calcined at 200 °C, only the surface and interlayer water is disposed, with the presence of the interlayer carbonate, so the uptake capacity of bromide ion is lower (30.8 mg/g). Upon further increasing the calcination temperature, carbonate is decomposed from interlayer region of LDHs, and the layered structure of LDHs transforms to aluminum and magnesium oxides which have higher capacity to rehydrate in aqueous medium. The interlayer carbonate of LDHs is decomposed completely when calcined at 500 °C. When the calcination temperature is above 500 °C, CLDH partly transformes into a spinel which does not exhibit the property of reconstruction, resulting in the observed decrease in the loading for anions (600 °C, 44.2 mg/g; 800 °C, 5.1 mg/g).

The effect of varying Mg/Al molar ratio on the removal of bromide ion was also investigated. It was found that the retention of bromide ion by the CLDH with Mg/Al molar ratio 4 is the best of all, reaching 94.0 mg/g, while the uptake capacity of

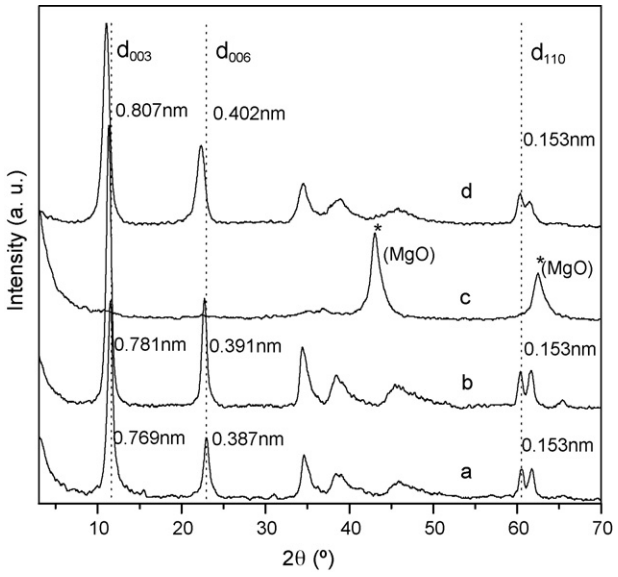

Fig. 1. Power XRD patterns for (a) MgAl-CO_3 LDH, (b) LDH after uptake of bromide ion, (c) CLDH and (d) CLDH after uptake of bromide ion.

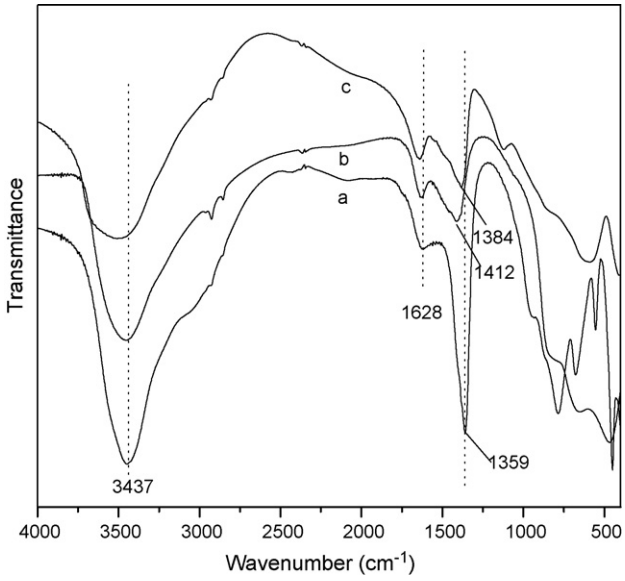

Fig. 2. FT-IR spectra for (a) MgAl-CO_3 LDH, (b) CLDH and (c) CLDH after uptake of bromide ion.

CLDH with Mg/Al ratios of 3 and 2 are 74.0 and 55.8 mg/g, respectively. This is attributed to the larger radius of bromide ion (0.196 nm), which is more suitable to lower charge density of slabs with an Mg/Al molar ratio of 4 than that of with 2 and 3.

The XRD pattern of the MgAl-CO_3 LDHs (Fig. 1a) shows sharp and symmetric peaks at lower 2θ values, which are characteristic of hydrotalcite-like compounds, and the material consists of a single crystalline phase [1]. However, the LDHs after uptake of bromide ion give a basal spacing of 0.780 nm (Fig. 1b), which is almost the same as that of LDHs precursor. Because the affinity of bromide ion towards LDHs is much lower than that of carbonate, the ion-exchange of bromide ion for carbonate in LDHs interlayer is difficult. As a result, the uptake of bromide by MgAl-CO_3 LDHs mainly occurs on the surface of LDHs. After the MgAl-CO_3 LDHs was calcined at 500 °C the layered hydrotalcite-like structure is absent (Fig. 1c), leading to the formation of a mixed magnesium aluminum oxide. However, rehydration of CLDH (Fig. 1d) has been observed to take place after bromide ion adsorption, giving a material with basal spacing of 0.802 nm, which is larger than that for MgAl-CO_3 LDHs as precursor (0.769 nm) and similar to that of Br-HTlc (0.795 nm) [1]. This indicates that the formation of MgAl-Br LDHs.

The FT-IR spectrum of the MgAl-CO_3 LDHs precursor shows a band at 1359 cm^{-1} (see Fig. 2a) attributed to the absorption of CO_3^{2-}, as reported previously [1]. It can be seen in Fig. 2b that the bands between 400 and 800 cm^{-1} could be due to the superposition of the vibrational absorptions of magnesium and aluminum oxides. The shoulders observed at 1628 and 1412 cm^{-1} are characteristic vibrational absorptions of reversibly adsorbed H_2O and CO_2 on oxide surfaces (Fig. 2b). After adsorption of bromide, the band at 1359 cm^{-1} shifts to higher frequency 1384 cm^{-1} (Fig. 2c). This could be due to the reconstruction of the layered material in the presence of bromide.

The TG–MS measurements (see Fig. 3A and B) show that the reconstructed LDHs has three stages of weight loss upon heating between 30 and 1100 °C: the first one from room temperature to 230 °C can be attributed to the removal of surface adsorbed water and interlayer water molecules according to MS spectrum of H_2O (*m/z* 18) (Fig. 3B), corresponding to the endothermic peak at 212 °C in the DTA curve (Fig. 3A); the second step (230–500 °C), involving a gradual weight loss, is the result of the deintercalation of carbonate (MS:*m/z* 44 (CO_2), 392 °C) and dehydroxylation of the brucite-like layers ((MS:*m/z* 18 (H_2O), 413 °C), and meanwhile the bromide ion of interlayer has also been observed by MS, corresponding to the endothermic peak at 401 °C in the DTA curve; the third step (500-1100 °C) is assigned to the deintercalation of bromide ion (MS:*m/z* 79 (Br), 80 (Br) and 81 (HBr)), corresponding to the endothermic peak at 900 °C.

Chemical analysis indicates that the material formed after reaction of CLDH with bromide has an Mg/Al molar ratio of 4.15:1, close to that of both the LDHs precursor (4.12:1) and CLDH (4.08:1).

Base on the results above, it can be concluded that the uptake capacity of bromide ion by CLDH is higher than that of LDHs precursor, due to their different uptake mechanism. The former is based on the reconstruction which the calcined product CLDH ($Mg_{0.80}Al_{0.20}O_{1.1}$) can be rehydrated with incorporation of bromide, to reform a layered structure. And the latter is due to surface adsorption. Therefore, LDHs calcined at 500 °C with Mg/Al molar ratio of 4 was chosen to carry out the experiments in the following section.

4.2. Effect of dosage of CLDH

The effect of the dosage of adsorbent on the uptake of bromide with initial concentration of 100 mg/L was studied, and the results are shown in Fig. 4. It can be seen that the amount of

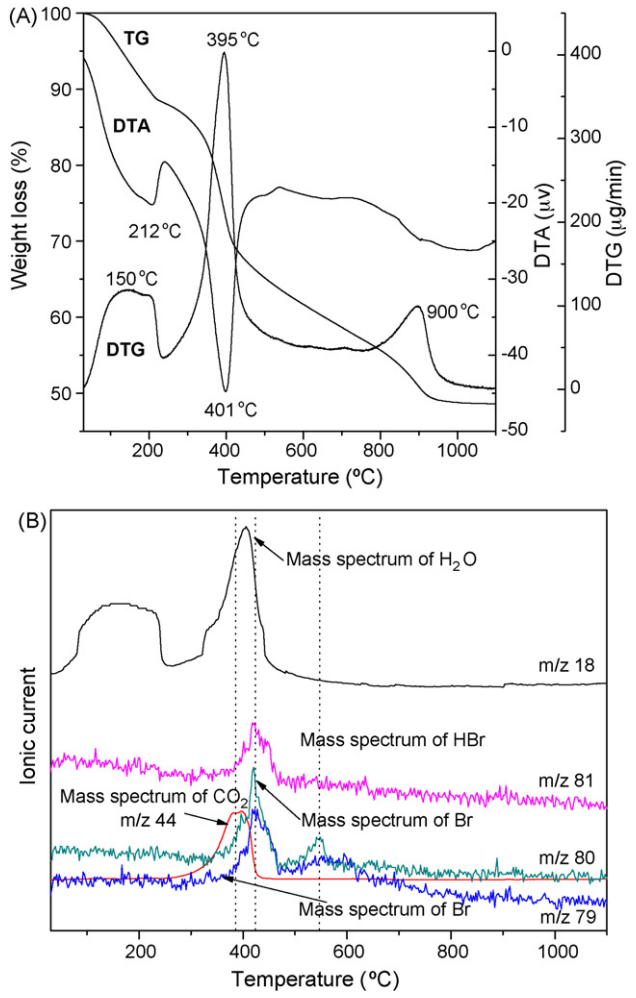

Fig. 3. TG–MS profiles for CLDH after uptake of bromide ion. (A) TG-DTA and (B) MS.

adsorbent significantly influenced the removal of bromide. The percentage removal of bromide was 73.4% for 0.2 g/L of CLDH, while it greatly increased to 91.6% for 1.0 g/L of adsorbent. However, there was only a small change in the extent of bromide adsorption when the dosage of adsorbent was over 1.0 g/L. For example, the percentage removal was 93.9% for 4.0 g/L of adsorbent.

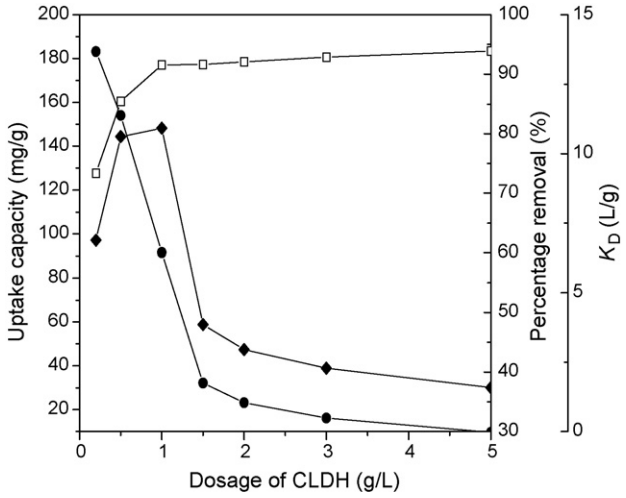

Fig. 4. Effect of dosage of CLDH on the uptake of bromide ion. (●) uptake capacity vs. dosage of CLDH; (□) percentage removal vs. dosage of CLDH; (♦) distribution coeffient K_D vs. dosage of CLDH.

Furthermore, the higher adsorbent dose results in lower adsorption capacity of CLDH at a fixed bromide concentration (100 mg/L), as shown in Fig. 4. This is consistent with the argument that the surface sites of the adsorbent are heterogeneous [30]. The distribution coefficient K_D increases with increasing adsorbent dose in the range 0.2–1.0 g/L while decreases with increasing adsorbent dose in the range 1.0–4.0 g/L (see Fig. 4), which also implies that the surface of CLDH is heterogeneous. If the surface is homogeneous, the K_D values should not change with adsorbent concentration.

4.3. Equilibrium isotherms

Fig. 5A is the equilibrium isotherms of bromide on CLDH at different temperature, which indicates that the uptake capacity increases upon increasing equilibrium concentration of bromide and decreasing temperature. The observation shows that the interaction between adsorbate and adsorbent is exothermic in nature, even though the change in the temperature does not influence the equilibrium time and the removal curve is smooth and continuous.

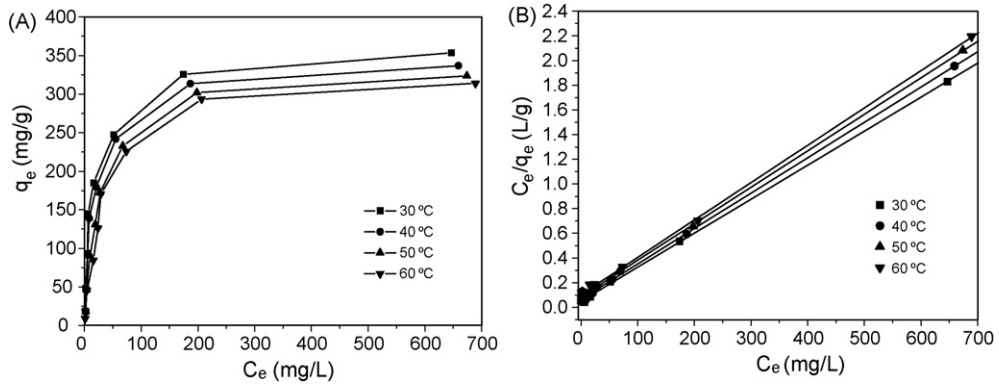

Fig. 5. Equilibrium isotherms for the uptake of bromide ion by CLDH. (A) Equilibrium isotherms and (B) Langmuir fitting.

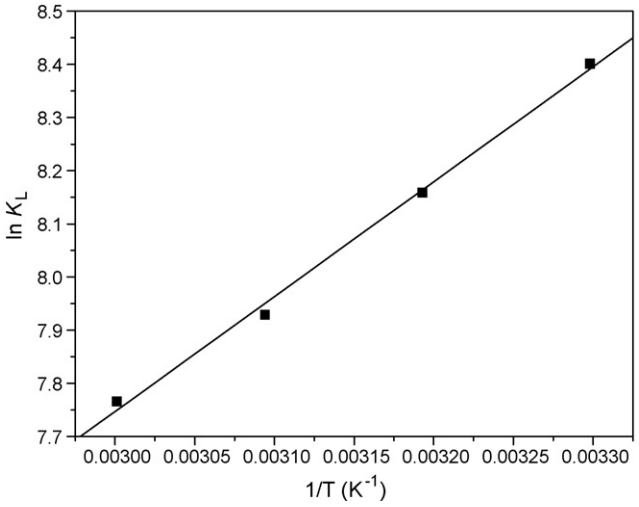

Fig. 6. Van't Hoff plot for uptake of bromide ion by CLDH.

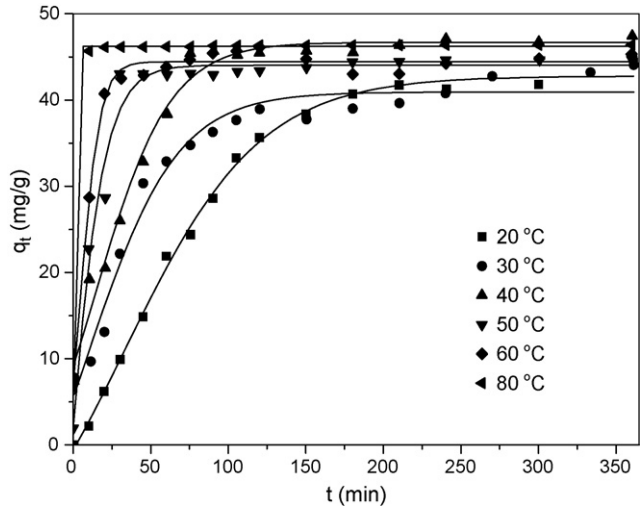

Fig. 7. kinetics and effect of temperature on the uptake of bromide ion by CLDH. (V = 2 L, [Br^-] = 50 mg/L, [CLDH] = 1.0 g/L).

The data were further analyzed by the Langmuir and Freundlich equations, respectively, and it was found that the Langmuir model gave a satisfactory fit to the experimental data, as shown in Fig. 5B and Table 1.

Thermodynamic parameters such as Gibbs free energy (ΔG^0), standard enthalpy change (ΔH^0), and standard entropy change (ΔS^0) for the process were calculated using the equations:

$$\Delta G^0 = -RT \ln K_L \quad (11)$$

$$\ln K_L = \frac{\Delta S^0}{R} - \frac{\Delta H^0}{RT} \quad (12)$$

where R is universal gas constant, T is temperature (K), and K_L is Langmuir constant. The values of ΔG^0, ΔH^0 and ΔS^0 are also listed in Table 1. The negative ΔG^0 value indicates the spontaneity of the removal of bromide process. ΔH^0 and ΔS^0 were calculated from a Vant' Hoff plot (see Fig. 6, correlation coefficient R^2 = 0.999) using the slope and intercept by regression method, respectively. The negative value of ΔH^0 confirms the exothermic nature of uptake of bromide by CLDH which has been predicted earlier from Fig. 5A. The negative value of ΔS^0 suggests the decreased randomness at the solid/solution interface for the removal of bromide on CLDH because of its reconstruction to Br-LDHs.

4.4. Uptake kinetics

Temperature is a highly significant parameter in the adsorption process. Fig. 7 displays the adsorption curves obtained under different isothermal conditions. The rate of adsorption increases significantly while the time taken to reach equilibrium decreases with the increase of temperature, and whether this is due to a chemical reaction or diffusion control mechanism will be discussed later. Fig. 8.

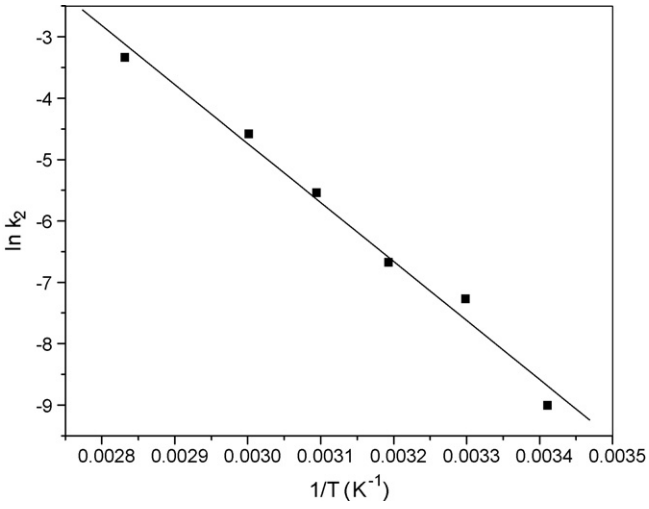

Fig. 8. Arrhenius plots for uptake of bromide ion by CLDH.

Table 2 presents the results of fitting experimental data to first order, pseudo-second order and intraparticle diffusion models, respectively. It can be seen from Table 2 that the correlation coefficient (R^2) varies in the order: pseudo-second order > intraparticle diffusion > first order model under all exper-

Table 1
Langmuir constants and thermodynamic parameters associated with bromide ion removal onto CLDH

Temperature (°C)	q_m (mg/g)	K_L (L/mol)	ln K_L	ΔG^0 (kJ/mol)	ΔH^0 (kJ/mol)	ΔS^0 (J/mol/K)
30	362.3	4452.5	8.401	−21.18	−17.96	−10.52
40	348.4	3495.7	8.159	−21.25		
50	337.8	2776.1	7.929	−21.31		
60	330.0	2359.4	7.766	−21.51		

Table 2
Experimental conditions, kinetic parameters and regression coefficients (R^2) for the three kinetic models

Run no.	$[Br^-]_0$ (mg/L)	[CLDH] (g/L)	Temperature (°C)	$q_{e,exp}$ (mg/L)	Fist order			Pseudo-second order			Intraparticle diffusion	
					$q_{e,cal}$ (mg/g)	$k_1 \times 10^{-2}$ (min^{-1})	R^2	$q_{e,cal}$ (mg/g)	$k_2 \times 10^{-4}$ (g/mg min)	R^2	k_i (mg/g min)	R^2
1	50	1.0	20	49.01	50.04	1.05	0.977	63.65	1.23	0.926	4.31	0.991
2	50	1.0	30	48.23	39.81	1.32	0.908	47.01	6.97	0.992	3.96	0.923
3	50	1.0	40	46.42	39.87	2.49	0.954	49.78	12.67	0.996	4.57	0.973
4	50	1.0	50	46.40	44.59	6.33	0.768	45.56	39.31	0.999	7.59	0.968
5	50	1.0	60	45.60	24.92	5.05	0.855	45.05	102.76	0.999	8.53	0.998
6	50	1.0	80	45.49	25.71	23.8	0.761	46.49	356.18	0.999	10.84	0.998

Table 3
Relationship between the bromide removal capacity and the number of regeneration cycles

Cycle number	1	2	3	4	5
Bromide removal capacity (mg/g)	91.6	91.3	90.7	90.9	89.7

$T = 30\,°C$, $[Br^-] = 100$ mg/L and [CLDH] = 1.0 g/L.

imental conditions, which indicates that the pseudo-second order model is the most satisfactory in describing the uptake kinetics of bromide on CLDH. The experimental q_e values agree well with the calculated ones obtained from the pseudo-second order kinetics model. The pseudo-second order equation is based on the uptake capacity of the solid phase and is in agreement with a chemisorption mechanism being the rate-determining step. Another advantage of the pseudo-second order model is that it predicts the behavior over the whole range of the adsorption process.

An Arrhenius plot (not shown here) of the adsorption rate against the reciprocal temperature was performed using the kinetic data of Table 2, giving a reasonably straight line ($R^2 = 0.990$). The gradient of this plot is $-(E_a/R)$, according to the well-known Arrhenius expression given in Eq. (13), and the activation energy can thus be calculated:

$$k_2 = A\,e^{-(E_a/RT)} \tag{13}$$

For diffusion-controlled processes, the activation energy of adsorption is lower than 20 kJ/mol. The calculated E_a value in our case, 79.9 kJ/mol, indicates that the process of bromide removal is controlled by the reaction rate of bromide with the CLDH rather than diffusion.

4.5. Regeneration and recycling studies

In order to recycle the adsorbent, it is necessary to regenerate the LDHs resulting. The regeneration studies were carried out using Na_2CO_3 aqueous solution (0.1 M). The mixture was stirred for 6 h, and the resulting solid was then filtered, washed thoroughly with deionized water, and calcined in a muffle furnace at 500 °C for 3 h. As can be seen from Table 3, the CLDH regenerated five times keep the almost same capacity to uptake bromide as a fresh one. So it can be concluded that the uptake of bromide is a reversible process, thereby facilitating the recycling of the material for further use.

5. Conclusions

The CLDH reconstructed to Br-LDHs after uptake of bromide, even as we expected, which is known as merry effect. The uptake capacity of LDHs precursor is lower than that of CLDH, due to their different uptake mechanism. The percentage removal of bromide increased upon increasing dosage of CLDH. The uptake capacity of CLDH increased with increasing equilibrium concentration of bromide and decreasing temperature. Thermodynamic parameters such as ΔG^0, ΔH^0, and ΔS^0 for the process were calculated from Langmuir constants. The pseudo-second order model is the most satisfactory in describ-

ing the adsorption kinetics of bromide on CLDH. E_a value was calculated to be 79.9 kJ/mol, using the kinetic data, indicating that the process of bromide removal is controlled by the reaction rate of bromide with the CLDH rather than diffusion.

Acknowledgements

This work was supported by the National Natural Science Foundation (No. 90306012), the Natural Science Foundation of Zhejiang Province (Y406345) and the Science and Technology Department of Quzhou City.

References

[1] F. Cavani, F. Trifiro, A. Vaccari, Hydrotalcite-type anionic clays: preparation, properties and applications, Catal. Today 11 (1991) 173–301.
[2] S. Miyata, Physico-chemical properties of synthetic hydrotalcites in relation to composition, Clays Clay Miner. 28 (1980) 50–56.
[3] Y.W. You, H.T. Zhao, G.F. Vance, Adsorption of dicamba (3,6-dichloro-2-methoxy benzoic acid) in aqueous solution by calcined-layered double hydroxide, Appl. Clay Sci. 21 (2002) 217–226.
[4] D.P. Das, J. Das, K. Parida, Physicochemical characterization and adsorption behavior of calcined Zn/Al hydrotalcite compound (HTlc) towards removal of fluoride from aqueous solution, J. Colloid Interface Sci. 261 (2003) 213–220.
[5] C. Diaz-Nava, M. Solache-Rios, M.T. Olguin, Sorption of fluoride ions from aqueous solutions and well drinking water by thermally treated hydrotalcite, Sep. Sci. Technol. 38 (2003) 131–147.
[6] N.K. Lazaridis, D.D. Asouhidou, Kinetics of sorptive removal of chromium (VI) from aqueous solutions by calcined Mg–Al–CO_3 hydrotalcite, Water Res. 37 (2003) 2875–2882.
[7] L. Lv, J. He, M. Wei, D.G. Evans, X. Duan, Uptake of chloride ion from aqueous solution by calcined layered double hydroxides: Equilibrium and kinetic studies, Water Res. 40 (2006) 735–743.
[8] L. Lv, J. He, M. Wei, D.G. Evans, X. Duan, Factors influencing the removal of fluoride from aqueous solution by calcined Mg–Al–CO_3 layered double hydroxides, J. Hazard. Mater. B 133 (2006) 119–128.
[9] L. Lv, J. He, M. Wei, D.G. Evans, Z.L. Zhou, Treatment of high fluoride concentration water by MgAl-CO_3 layered double hydroxides: Kinetic and equilibrium studies, Water Res. 41 (2007) 1534–1542.
[10] R.S. Magazinovic, B.C. Nicholson, D.E. Mulcahy, D.E. Davey, Bromide levels in natural waters: its relationship to levels of both chloride and total dissolved solids and the implications for water treatment, Chemosphere 57 (2004) 329–335.
[11] T. Myllykangas, T.K. Nissinen, J. Mäki-Paakkanen, A. Hirvonen, T. Vartiainen, Bromide affecting drinking water mutagenicity, Chemosphere 53 (2003) 745–756.
[12] W.R. Haag, J. Holgne, Ozonation of bromide-containing waters: kinetics of formation of hypobromous acid and bromate, Environ. Sci. Technol. 17 (1983) 261–267.
[13] U. Gunten, Y. Oliveras, Advanced oxidation of bromide-containing waters: bromate formation mechanisms, Environ. Sci. Technol. 32 (1998) 63–70.
[14] P. Rantakokko, T. Nissinen, T. Vartiainena, Determination of bromide ion in raw and drinking waters by capillary zone electrophoresis, J. Chromatogr. A 839 (1999) 217–225.
[15] M. Siddiqui, W. Zhai, G. Amy, C. Mysore, Bromate ion removal by activated carbon, Water Res. 30 (1996) 1651–1660.
[16] T. Nobukawa, S. Sanukida, Effect of bromide ions on genotoxicity of halogenated by products from chlorination of humic acid in water, Water Res. 35 (2001) 4293–4298.
[17] C.J. Johnson, P.C. Singer, Impact of a magnetic ion exchange resin on ozone demand and bromate formation during drinking water treatment, Water Res. 38 (2004) 3738–3750.
[18] T.H. Boyer, P.C. Singer, Bench-scale testing of a magnetic ion exchange resin for removal of disinfection by-product precursors, Water Res. 39 (2005) 1265–1276.
[19] X. Duan, Q.Z. Jiao, L. Li, New method of synthesis the uniform dispersion and superfine layered double hydroxides. CN 1288076, 2001-03-21.
[20] L.L. Ren, J. He, D.G. Evans, X. Duan, R.Y. Ma, Some factors affecting the immobilization of penicillin G acylase on calcined layered double hydroxides, J. Mol. Catal. B: Enzym. 16 (2001) 65–71.
[21] S. Lagergren, About the theory of so-called adsorption of soluble substances, K. Svenska Vetenskapsad. Handl. 24 (1898) 1–39.
[22] C. Namasivayam, K. Kadirvelu, Uptake of mercury (II) from wastewater by activated carbon from an unwanted agricultural solid by-product: coirpith, Carbon 37 (1999) 79–84.
[23] C.W. Cheung, J.F. Porter, G. McKay, Sorption kinetics for the removal of copper and zinc from effluents using bone char, Sep. Purif. Technol. 19 (2000) 55–64.
[24] N. Chiron, R. Guilet, E. Deydier, Adsorption of Cu(II) and Pb(II) onto a grafted silica: isotherms and kinetic models, Water Res. 37 (2003) 3079–3086.
[25] Y.S. Ho, G. Mckay, Sorption of dye from aqueous solution by peat, Chem. Eng. J. 70 (1998) 115–124.
[26] C. Namasivayam, S. Sumithra, Adsorptive removal of catechol on waste Fe(III)/Cr(III) hydroxide: equilibrium and kinetics study, Ind. Eng. Chem. Res. 43 (2004) 7581–7587.
[27] S.J. Allen, G. McKay, K.Y.H. Khader, Intraparticle diffusion of a basic dye during adsorption onto sphagnum peat, Environ. Pollut. 56 (1989) 39–50.
[28] Q. Sun, L.Z. Yang, The adsorption of basic dyes from aqueous solution on modified peat-resin particle, Water Res. 37 (2003) 1535–1544.
[29] M. Jansson-Charrier, E. Guibal, J. Roussy, Vanadium sorption by chitosan: kinetics and equilibrium, Water Res. 30 (1996) 465–475.
[30] X.P. Liao, B. Shi, Adsorption of fluoride on zirconium (IV)—impregnated collagen fiber, Environ. Sci. Technol. 39 (2005) 4628–4632.